NRC Publications Archive
Archives des publications du CNRC

Physical and electrochemical properties of some phosphonium-based ionic liquids and the performance of their electrolytes in lithium-ion batteries

Salem, Nuha; Zavorine, Serguei; Nucciarone, Donato; Whitbread, Kristina; Moser, Mike; Abu-Lebdeh, Yaser

NRC Publications Record / Notice d'Archives des publications de CNRC:
https://nrc-publications.canada.ca/eng/view/object/?id=d90d3706-0fc2-43d1-a551-967e3c06fa3a
https://publications-cnrc.canada.ca/fra/voir/objet/?id=d90d3706-0fc2-43d1-a551-967e3c06fa3a

National Research Council Canada   Conseil national de recherches Canada

Canada

Physical and Electrochemical Properties of Some Phosphonium-Based Ionic Liquids and the Performance of Their Electrolytes in Lithium-Ion Batteries

Nuha Salem,[a] Serguei Zavorine,[b,z] Donato Nucciarone,[b] Kristina Whitbread,[b] Mike Moser,[b] and Yaser Abu-Lebdeh[a,z]

[a]*National Research Council of Canada, Ottawa, Ontario K1A 0R6, Canada*
[b]*Solvay, Niagara Falls, Ontario L2E 6S5, Canada*

In this work, three ionic liquids with two different cations and two different anions: trimethyl propyl phosphonium bis-fluorosulfonyl imide (P_{1113}FSI), trimethyl isobutyl phosphonium bis-fluorosulfonyl imide (P_{111i4}FSI) and trimethyl isobutyl phosphonium bis-trifluoromethylsulfonyl imide (P_{111i4}TFSI) have been characterized and evaluated as electrolytes in lithium ion half-cells. It is found that ionic liquids with FSI^- anion have superior properties over their $TFSI^-$ counterparts and those with the smaller cation, P_{1113}, have better conductivity and viscosity. The two ionic liquids with FSI anion, P_{1113}FSI and P_{111i4}FSI, are liquid at room temperature and show high conductivities and low viscosities, reaching 10.0 mS/cm and 30 cP at room temperature for P_{1113}FSI. They also exhibit electrochemical windows higher than 5 V and thermal stability exceeding 300°C. Mixing the ionic liquids with 0.5 M $LiPF_6$ increases viscosities, lowers conductivities but improves electrochemical cathodic stability. The electrolyte mixtures have been evaluated in graphite/Li half cells, Li/LiFePO$_4$ and Li/LiMn$_{1.5}$Ni$_{0.5}$O$_4$ at C/12 for 100 cycles and at different rates: C/6, C/3, C and 2C for rate capabilities. Battery testing shows that unlike their $TFSI^-$ counterparts both ionic liquids with FSI^- anion perform well with graphite anode and LiFePO$_4$ cathode but fail with the higher voltage LiMn$_{1.5}$Ni$_{0.5}$O$_4$ cathode.

Li-ion batteries have attracted a lot of attention since their successful application in portable consumer electronics mainly because of their unique properties such as high energy density and long cycle life. Since then, and due to increased market demand, interest has been drawn toward investigating Li-ion batteries as candidates for use in more energy-demanding applications such as electric vehicles (EV, HEV, PHEV) and large energy storage systems for the electrical grid.[1–5] One important aspect of such investigation is to develop new and improved materials for Li-ion batteries to enhance their properties in terms of safety and performance, which is crucial to match the new demand. There have been a large number of studies on the anode, cathode and electrolyte components of Li-ion batteries for this purpose in recent years. Electrolyte solutions used in Li-ion batteries are usually composed of a lithium salt ($LiPF_6$) dissolved in a mixture of two or more carbonate solvents such as ethylene carbonate (EC) and dimethyl carbonate (DMC).[6] These solvents are known to have safety concerns due to their flammability, volatility and reactivity to other battery components prompting an increased effort on finding safer alternatives.[7] In the last decade, a group of compounds called ionic liquids (ILs), has been of interest as an alternative to conventional battery electrolytes due to their excellent thermal and physiochemical properties such as non-flammability, negligible vapor pressure, good dissolution power, good electrochemical stability, wide liquid range and intrinsic ionic conductivity.[7–13] Despite these aforementioned properties, some ILs suffer from poor cathodic stability, very high viscosity, incompatibility with other active and inactive battery components, impurities and high cost which make their application as electrolytes a challenging task.[14] However, the right combination between a certain cation and anion (which can produce a huge number of possible ILs) can result in an IL that has the desired properties for an electrolyte for Li-ion batteries.

Ionic liquids based on imidazolium, ammonium and phosphonium cations are the most commonly studied with the anion being, in most cases, trifluoromethanesulfonyl imide ($TFSI^-$), fluorosul-fonyl imide (FSI^-) and to less extent PF_6^-.[15,16] In this study, we present the physical and electrochemical properties of three ionic liquids based on phosphonium cations with different alkyl chain sizes and two different anions, trimethyl propyl phosphonium bis-fluorosulfonyl imide (P_{1113}FSI), trimethyl isobutyl phosphonium bis-fluorosulfonyl imide (P_{111i4}FSI) and trimethyl isobutyl phosphonium bis-trifluoromethylsulfonyl imide (P_{111i4}TFSI) (Scheme 1).

While some labs have already investigated the properties of some of these ionic liquids and their electrolytes formulated with LiFSI salt,[17,18] we formulated our electrolytes with $LiPF_6$, the dominant salt in commercial rechargeable lithium-ion batteries (LIBs) based on a graphite anode and a 3–4 V cathode material.

Lastly, none of the previous studies investigated the battery performance in details such as long-term cycling and rate capabilities with cathode, especially the high voltage ($\sim$ 5V) LiMn$_{1.5}$Ni$_{0.5}$O$_4$ cathode, and graphite anode material as has been done in the present investigation.

Experimental

Ionic liquids.—Ionic liquids were provided by Solvay with purity of >96% for P_{1113}FSI and >99% for P_{111i4}FSI and P_{111i4}TFSI and were additionally dried overnight in vacuum oven at 80°C before they were characterized and used in battery testing.

Water content of <50 ppm was measured using Karl-Fischer MCI moisture meter, model CA-05 from Mitsubishi.
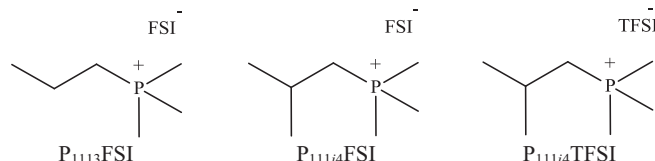
Scheme 1. Chemical structure of the three phosphonium-based ionic liquids used in this work.

[z]E-mail: Yaser.Abu-Lebdeh@nrc.gc.ca; Serguei.Zavorine@solvay.com

Thermal and electrochemical characterization.—Differential scanning calorimetry (DSC) analysis was recorded using a TA Instruments DSC Q2000. All samples were sealed in aluminum pans inside an Ar-filled glove box and then scanned from −90 to 150°C at a rate of 5°C/min under helium gas. Conductivity measurements were performed using the AC impedance spectroscopy technique where the electrolyte solutions were poured into a two-platinum-electrode conductivity cell with a cell constant of 1 cm^{-1}. The frequency was swept between 1 kHz and 0.1 Hz using Princeton Applied Research PAR 263A potentiostat coupled with a Solartron frequency response analyzer FRA 1255B. The temperature was varied between −20 and 100°C allowing 20 min for thermal equilibration. Linear sweep voltammograms were conducted using a platinum microelectrode (25 μm) and a silver wire as a counter and reference electrode. These measurements were also done using the Princeton Applied Research PAR 263A potentiostat at room temperature with a scan rate of 10 mV/s.

Viscosity.—Viscosity measurements were recorded using a CANNON-Ubbelohde viscometer. This method requires a sample size of 7–9 ml and for this reason the viscosity of 0.5 M LiPF$_6$ P$_{1113}$FSI was not determined due to insufficient amount.

Half-cell assembly.—Battery investigations were carried out with coin-type cells. Cathode was made from a slurry containing 80% LiFePO$_4$ (in-house synthesized) or LiMn$_{1.5}$Ni$_{0.5}$O$_4$ (NEI corporation), 5% KS-4 graphite, 5% Super-P carbon and 10% PVDF binder in NMP and anode was made of 85% MCMB graphite, 5% Super-P carbon and 10% PVDF binder in NMP. The cathode slurry was casted onto an aluminum foil while the anode slurry was coated on copper foil then dried overnight at 80°C in a vacuum oven. Electrode discs of 12.7 mm diameter were punched from the coated foil and pressed at 0.5 ton pressure. The cells were assembled in an Ar-filled dry box at room temperature using Li as anode and 2 layers of microporous polypropylene separators (Celgard 3501). Cell performance was evaluated by galvanostatic experiments carried out on a multichannel Arbin battery cycler at 30°C. Li/LiFePO$_4$ and MCMB/Li half cells were cycled at 2.5–4.2 V and 0.005–1.5 V respectively. The cells were charged and discharged at constant current density of C/12 for long term cycling and at C/6, C/3, C and 2C (10 cycles each) for rate capabilities.

Results and Discussion

Characterization of ionic liquids.—*Differential scanning calorimetry.*—DSC scans of the three neat ionic liquids and their corresponding electrolyte solutions with LiPF$_6$ salt were recorded from −90°C to 150°C as seen in Figure 1. It can be seen that the melting points (m.p.) of the three liquid salts, P$_{1113}$FSI, P$_{111i4}$FSI and P$_{111i4}$TFSI in their neat form were: 2.4°C, 12.5°C (liquids at room temperature) and 43°C (solid at room temperature), respectively. The first two values were in agreement with Tsunashima *et al.*[17] and Girard et al.[18] while the last value was in agreement with Hilder et al.[19] As expected, the TFSI$^-$-based ILs have higher m.p. than the FSI-based analogs.[20] These values illustrate the crucial effect of the size and shape of the cation in combination with the size and shape of the anion on the packing and crystallization behavior of the salt.[21] It was also observed that P$_{1113}$FSI was the only ionic liquid that showed extra peaks below melting that can be attributed to the presence of other phases/crystalline structures of lower melting points or due to a solid-solid transition corresponding to a regular crystalline to plastic crystalline phase.[22] When LiPF$_6$ salt was added (to the molten state in case of P$_{111i4}$TFSI), the m.p. was expectedly shifted to much lower values: <−90°C for 0.5 M LiPF$_6$ P$_{1113}$FSI, 0.5°C for 0.5 M LiPF$_6$ P$_{111i4}$FSI and 17–23°C for 0.5 M LiPF$_6$ P$_{111i4}$TFSI. The negative shift in the melting point upon adding the lithium salt is expected and usually attributed to the disruptive effect the salt has on the packing of ionic liquid molecules due to the new strong ion-ion interactions between the ionic liquid and the lithium salt ions.
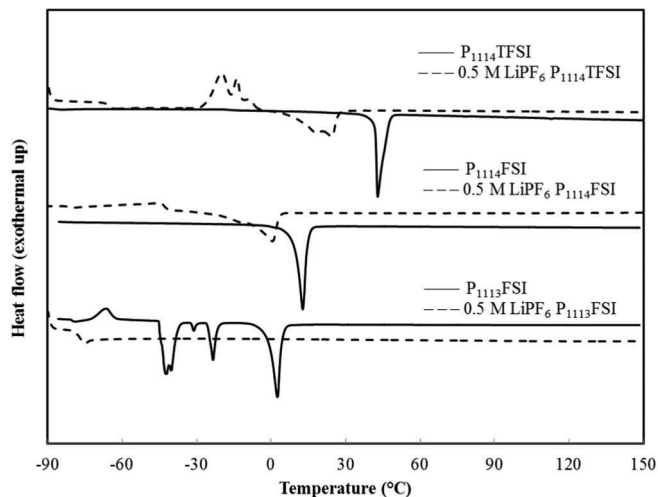

Figure 1. Differential scanning calorimetry of the neat ionic liquids (solid line) and their electrolytes (dashed line). P$_{1114}$FSI and P$_{1114}$TFSI refer to P$_{111i4}$FSI and P$_{111i4}$TFSI in the text.

Viscosity and conductivity.—The viscosity of neat P$_{1113}$FSI and P$_{111i4}$FSI liquids were measured at room temperature and found to be 30 and 40 cP, respectively, while the viscosity of P$_{111i4}$TFSI was not determined because it's a solid state at room temperature. These values are in agreement with the values determined by Tsunashima et al.[17] and Girard et al.[18] The viscosity of ionic liquids is known to depend, among other things, on the molecular frictional forces that are governed by their size. It is known that molecules with high molecular weight show higher friction along with slow diffusion and therefore lead to higher viscosity.[21–23] This explains the increase of viscosity as the cation becomes bigger (P$_{111i4}$>P$_{1113}$). Upon the addition of the 0.5 M LiPF$_6$ to P$_{111i4}$FSI, the viscosity increased to 91 cP due to the introduction of much stronger ion-ion interactions, e.g. FSI$^-$ and Li$^+$.[24] The viscosity of 0.5 M LiPF$_6$ P$_{1113}$FSI, which was not determined due to insufficient amount of material, was also visibly higher (qualitatively) than the neat P$_{1113}$FSI but lower than 0.5 M LiPF$_6$ P$_{111i4}$FSI, as expected. To compare the effect of the anion on the viscosity of the electrolyte, 0.5 M LiPF$_6$ P$_{111i4}$TFSI was prepared by adding the lithium salt to the molten ionic liquid. The electrolyte did not solidify upon cooling, as evident from DSC, which showed a melting point just below room temperature. This is attributed, as mentioned above, to the disruption of the interaction between P$_{111i4}$ cation and TFSI$^-$ anion due to the new interaction with the smaller Li$^+$ cation from LiPF$_6$. The viscosity of 0.5 M LiPF$_6$ P$_{111i4}$TFSI, however, was high at 269 cP. Although the comparison to the neat P$_{111i4}$TFSI viscosity is not possible at room temperature, it can be seen here that the ion-ion interaction between TFSI$^-$ and Li$^+$ is much stronger than FSI$^-$ and Li$^+$. This explains the much higher viscosity of the LiPF$_6$ electrolyte of the TFSI$^-$ ionic liquid compared to its FSI$^-$ counterpart.[24,25]

The ionic conductivities of the neat ionic liquids and their electrolytes with LiPF$_6$ were measured over a temperature range from −20 to 100°C (40 to 100°C for P$_{111i4}$TFSI) as shown in Figure 2. It was found that for neat ionic liquids the trend in conductivity at any given temperature followed, inversely, the trend in viscosity as follows: P$_{1113}$FSI >P$_{111i4}$FSI >P$_{111i4}$TFSI. It was also found that the conductivity increased as a function of temperature reaching 37.0 mS/cm, 27.0 mS/cm and 15.1 mS/cm at 100°C, respectively. The conductivity-temperature curve of P$_{111i4}$FSI showed a large drop in the conductivity at −20 and 0°C due to freezing at 12.5°C. On the other hand, P$_{1113}$FSI showed no such discontinuities due to, as shown by DSC, its partial melting at temperatures that extended to −50°C. It should also be noted that the value of the conductivity for P$_{1113}$FSI (10 mS/cm) is higher than the one reported by Tsunashima et al. (7.1 mS/cm) and we are currently unable to discern the reasons for such a difference.
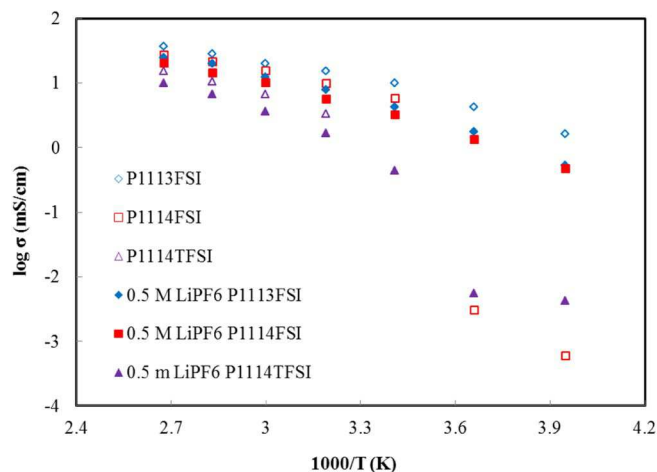
Figure 2. Conductivity as a function of temperature of neat ionic liquids (open symbols) and their electrolytes (filled symbols). P_{1114}FSI and P_{1114}TFSI refer to P_{111i4}FSI and P_{111i4}TFSI in the text.

Figure 3. Linear sweep scans vs Ag/Ag$^+$ of the neat ionic liquids (solid line) and their electrolytes (dashed line) using Pt working electrode and Ag wire as a pseudo reference electrode at scan rate of 10 mV/s. P_{1114}FSI and P_{1114}TFSI refer to P_{111i4}FSI and P_{111i4}TFSI in the text.

The addition of 0.5 M LiPF$_6$ decreased the conductivities due to the increased viscosity as expected with a trend matching the neat ionic liquids: 0.5 M LiPF$_6$ in P_{1113}FSI >0.5 M LiPF$_6$ P_{111i4}FSI >0.5 M LiPF$_6$ P_{111i4}TFSI. Room temperature conductivities of 4.8 mS/cm, 3.5 mS/cm and 0.55 mS/cm for 0.5 M LiPF$_6$ in P_{1113}FSI, P_{111i4}FSI and P_{111i4}TFSI, respectively, were lower than those for conventional carbonate-based electrolytes which are usually >8 mS/cm. The values for the two FSI$^-$ ionic liquid electrolytes, although lower than conventional electrolytes, are considered high in comparison to other ionic liquids with different cation/anion combinations. The focus on phosphonium-based ionic liquids has recently increased due to the fact that they usually exhibit lower viscosities and higher conductivities compared to their ammonium-based ionic liquid counterparts.[26] For example, P_{2225}TFSI was found to have a viscosity of 88 mPa.s while its ammonium counterpart, N_{2225}TFSI has a viscosity of 172 mPa.s.[26] It should be noted, however, that P_{1113}TFSI is a solid with m.p. of 40–43°C [17, 19, this study] while N_{1113}TFSI is a liquid with the viscosity of 72 cP and the conductivity of 3.3 mS/cm.[27]

It is conventional to say that ionic conductivity is inversely controlled by viscosity, but although this statement is empirically correct it is not from the theoretical point of view; as in essence both the conductivity and viscosity are controlled by similar forces. The addition of a salt to an ionic liquid can only increase the short-range, ion-ion coulombic interactions but there is evidence that, similar to other amorphous materials and glass-forming liquids (molten salts, polymer electrolytes, and ionic glass, concentrated liquid electrolytes), free volume, the free space surrounding molecules or ions in the liquid state, might be responsible for ion transport.[28] Recently, the original ideas of Doolittle and Cohen-Turnbull on free volume have been applied by Krause-Rehberg and coworkers to ionic liquid electrolytes and Abu-Lebdeh and co-workers to molecular liquid electrolytes and new relationships that correlate viscosity and conductivity to free volume have been introduced.[28,29] A correlation with the salt-solvent phase diagram has also been introduced in the case of molecular liquid electrolytes where the concentration of maximum conductivity was correlated to the eutectic composition,[29] Unfortunately this analysis is out of the scope of this work and will be reported separately, however it clearly demonstrates that there is little known about the structure and transport mechanism in both molecular and ionic liquid electrolytes.

Linear sweep voltammetry.—The electrochemical stability of the ILs was evaluated using linear sweep voltammetry and the results are shown in Figure 3. The anodic voltammetry sweep of the neat ionic liquids P_{1113}FSI and P_{111i4}FSI showed an oxidation onset at 2.42 V and 2.53 V (vs Ag/Ag$^+$), respectively, while cathodic voltammetry sweep showed an onset of reduction at −2.63 V and −2.9 V vs Ag/Ag$^+$ respectively. These values correspond to an electrochemical
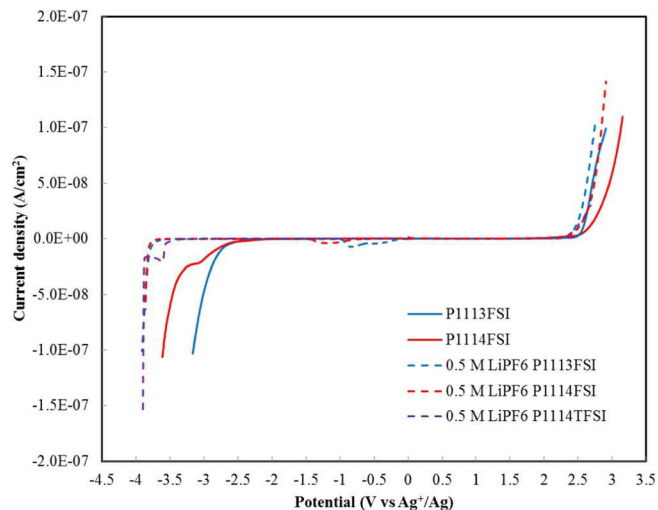
stability window of 5.05 V for P_{1113}FSI and 5.43 V for P_{111i4}FSI. Our results are in a good agreement with Tsunashima et al.[17] who found that P_{1113}FSI has a potential window of ∼ 5.0 V and Girard et al.[18] who found that P_{111i4}FSI has a potential window of 5.5 V with a slightly different oxidation and reduction onset in both cases. These slight differences could simply be attributed to a shift in potential due to the use of different electrodes and possibly due to different impurity profiles originating from two different synthetic methods. The higher cathodic stability of P_{111i4}FSI is attributed to the higher cathodic stability of the P_{111i4} cation due to the presence of the more electron donating, branched isobutyl group in comparison with linear n-propyl group.[30]

Upon the addition of 0.5 M LiPF$_6$, the cathodic stability was improved for P_{1113}FSI and P_{111i4}FSI by 1.2 V and 0.9 V, respectively, resulting in an electrochemical stability window of 6.25 V for 0.5 M LiPF$_6$ P_{1113}FSI and 6.33 V for 0.5 M LiPF$_6$ P_{111i4}FSI. This improvement is likely the result of the passivation caused by the reduction product of PF$_6$ anion.[31] It was possible to run the linear sweep of 0.5 M LiPF$_6$ P_{111i4}TFSI since the mixture was liquid and was found to have a reduction onset of −3.8 V and an oxidation onset of 2.5 V vs Ag/Ag$^+$. The slightly higher oxidation potential compared to 2.4 V for 0.5 M LiPF$_6$ P_{111i4}FSI vs Ag/Ag$^+$ is attributed to the better stability of TFSI$^-$ toward oxidation than FSI$^-$ due to higher charge delocalization.[32] The scans for the FSI$^-$ ionic liquids with LiPF$_6$ show small reduction peaks in the potential range from − 0.5 V to −1 V on the cathodic run, which can be attributed to impurities such as residual water that might have been introduced by the lithium salt.[33]

Battery performance.*—Graphite/Li half cells.*—Electrolyte mixtures based on each of the ionic liquids with 0.5 M LiPF$_6$ were prepared and used for battery testing. 0.5 M LiPF$_6$ was chosen to ensure complete solubility and maintain acceptable conductivity by keeping viscosity as low as possible. LiPF$_6$ also is significantly less expensive than LiTFSI and LiTSI salts. Figure 4a shows the cycling performance of MCMB/Li half cells formulated with these electrolytes and with 1 M LiPF6 EC/DMC 1:1 conventional electrolyte for comparison. Both 0.5 M LiPF$_6$ P_{1113}FSI and 0.5 M LiPF$_6$ P_{111i4}FSI produced capacities that are comparable to the conventional electrolyte with slightly higher initial discharge capacities of 363 mAh/g and 350 mAh/g, respectively, compared to 340 mAh/g for 1 M LiPF$_6$ EC/DMC 1:1 (v/v). The irreversible capacities, ∼ 30 mAh/g, were also comparable with conventional electrolyte. The capacities stabilized at 325 mAh/g for both electrolytes with no capacity loss for 0.5 M LiPF$_6$ P_{1113}FSI and 7% capacity loss for 0.5 M LiPF$_6$ P_{111i4}FSI over 100

Figure 4. (a) Discharge capacities of MCMB graphite/Li half-cells made with ionic liquid and conventional electrolytes at C/12. Open symbols are corresponding coulombic efficiencies. (b-d) Corresponding cycling performance curves at 1st and 10th cycles. (c) Corresponding cycling performance curves of 0.5 M LiPF$_6$ P$_{111i4}$FSI at 1st and 10th cycles. (d) Corresponding cycling performance curves of 0.5 M LiPF$_6$ P$_{111i4}$TFSI at 1st and 10th cycles. P$_{1114}$FSI and P$_{1114}$TFSI refer to P$_{111i4}$FSI and P$_{111i4}$TFSI in the text.
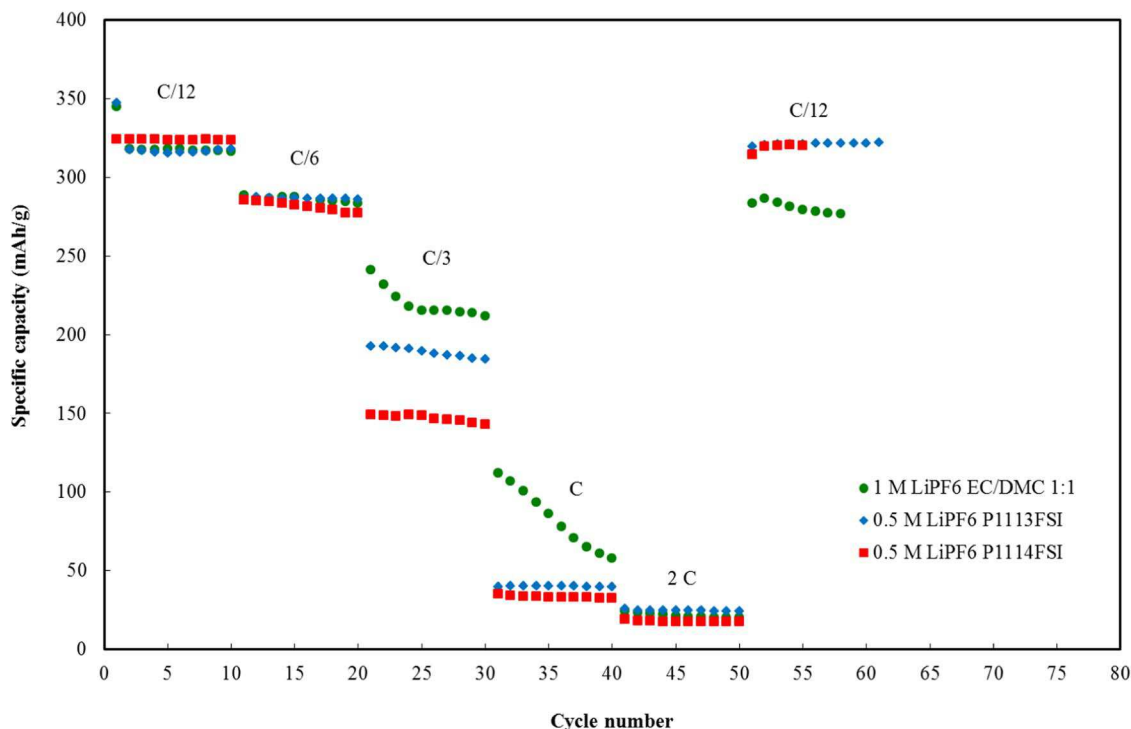
Figure 5. Rate capabilities of MCMB graphite/Li half-cells made with ionic liquid and conventional electrolytes at C/12, C/6, C/3, C and 2C. P_{1114}FSI refers to P_{111i4}FSI in the text.

cycles. The electrolyte made with 0.5 M LiPF$_6$ P_{111i4}TFSI, failed to cycle with MCMB/Li giving initial capacity of only 55 mAh/g which dropped to almost zero in the subsequent cycles. The inability of 0.5 M LiPF$_6$ P_{111i4}TFSI electrolyte mixture to give any capacity is attributed to its failure to form a functioning SEI layer as evidenced by the discharge/charge curve, as discussed below. The efficiencies of the two FSI electrolytes were excellent approaching 100% which indicate minimal energy loss during the charge-discharge cycling process. Charge-discharge curves of the 1st and 10th cycle for these half cells are shown in Figure 4b–4d. It can be seen from these curves that an SEI layer starts to form in the first cycle at 1 V for 0.5 M LiPF$_6$ P_{1113}FSI and 0.65 V for 0.5 M LiPF$_6$ P_{111i4}FSI due to the decomposition of the electrolyte. This decomposition disappears in the subsequent cycles indicating the formation of a stable SEI layer. In the case of 0.5 M LiPF$_6$ P_{111i4}TFSI, this step is much more pronounced, which indicates a higher degree of decomposition represented by a reduction activity that can be seen at -3.5 V in the linear sweep (Figure 3). This decomposition possibly leads to a thick, insulating SEI layer resulting in the irreversible intercalation/de-intercalation process and the poorer performance

Rate capabilities at faster charge-discharge rates of C/6, C/3, C and 2C were also investigated as seen in Figure 5. The performance of 0.5 M LiPF$_6$ P_{1113}FSI was better than 0.5 M LiPF$_6$ P_{111i4}FSI at C/3, C and 2C. Capacities were reasonable up to C/3: 190 mAh/g and 149 mAh/g for 0.5 M LiPF$_6$ P_{1113}FSI and 0.5 M LiPF$_6$ P_{111i4}FSI, respectively, but faded significantly at higher rates to <50 mAh/g. In general, the capacities at rates >C/6 were higher for conventional electrolyte than both ionic liquids. Lower rate capability behavior could be attributed to the lower conductivity of the ionic liquid solutions compared to the conventional electrolyte and most probably lower Li$^+$ transport numbers. The recovery at C/12 was however better for the ionic liquids compared to the conventional electrolyte.

Li/LiFePO$_4$ half cells.—Li/LiFePO$_4$ half-cells were made using the same electrolytes used in graphite/Li half cells. The cells gave an initial discharge capacity of 124 mAh/g and 110 mAh/g for 0.5 M LiPF$_6$ P_{1113}FSI and 0.5 M LiPF$_6$ P_{111i4}FSI, respectively, which

are lower than the one obtained with 1 M LiPF$_6$ EC/DEC 3:7 (v/v) conventional electrolyte (150 mAh/g) (Figure 6a). The capacities of the two electrolytes however reached maximum after 20 cycles and stabilized for the remaining 100 cycles. These capacities were slightly better for 0.5 M LiPF$_6$ P_{1113}FSI (152 mAh/g) compared to both 0.5 M LiPF$_6$ P_{111i4}FSI (147 mAh/g) and the conventional electrolyte (148 mAh/g). Both conventional and 0.5 M LiPF$_6$ P_{1113}FSI electrolytes lost only 4% of capacity over 100 cycles while 0.5 M LiPF$_6$ P_{111i4}FSI lost 11% of its capacity over 100 cycles. The coulombic efficiencies were irregular and in some cases poor reaching values as low as 92% for the FSI ionic liquid electrolytes for the first 12 cycles which then improved to $\sim$ 99% for the duration of the cycling. This poor efficiency could be attributed to higher polarization at the electrolyte-electrode interface due to slower diffusion in the electrolyte as a result of the higher viscosity exacerbated by the slow Li diffusion at the, FePO$_4$/LiFePO$_4$ two-phase region of the LFP electrode.[27] As expected, half-cells made with 0.5 M LiPF$_6$ P_{111i4}TFSI gave poor performance with initial capacities of only 85 mAh/g, which faded sharply to almost zero after 20 cycles. Charge-discharge curves of the 1st and 10th cycle for these half cells are shown in Figure 6b–6d. The cell with the FSI ionic liquids shows a plateau at 3.45 V corresponding to Fe^{+2}/Fe^{+3} redox couple reaction associated with lithium ion intercalation/de-intercalation with an irreversible capacity of 27 mAh/g and 39 mAh/g for 0.5 M LiPF$_6$ P_{1113}FSI and 0.5 M LiPF$_6$ P_{111i4}FSI in the first cycle respectively. After 10 cycles, the cells had excellent coulombic efficiency with minimal irreversible capacity. The plateau for 0.5 M LiPF$_6$ P_{111i4}TFSI occurs at higher voltage of 3.8 V indicating higher polarization due to higher viscosity, as discussed above. High irreversible capacity in the first cycle and poor cycling in the subsequent cycles can also be seen for this electrolyte.

Similar to graphite/Li half cells, the rate capabilities were evaluated by performing 10 cycles at C/6, C/3, C and 2C followed by recovery cycles at C/12, taking into account that 1 C rate for the Li/LFP cell corresponds to $\sim$C/3 for the graphite/Li cell. Both the FSI ionic liquid electrolytes behaved in a similar manner, as shown in Figure 7. The capacities at C/6 and C/3 were very good for electrolytes, 145 mAh/g and 140 mAh/g respectively, being higher than for the conventional

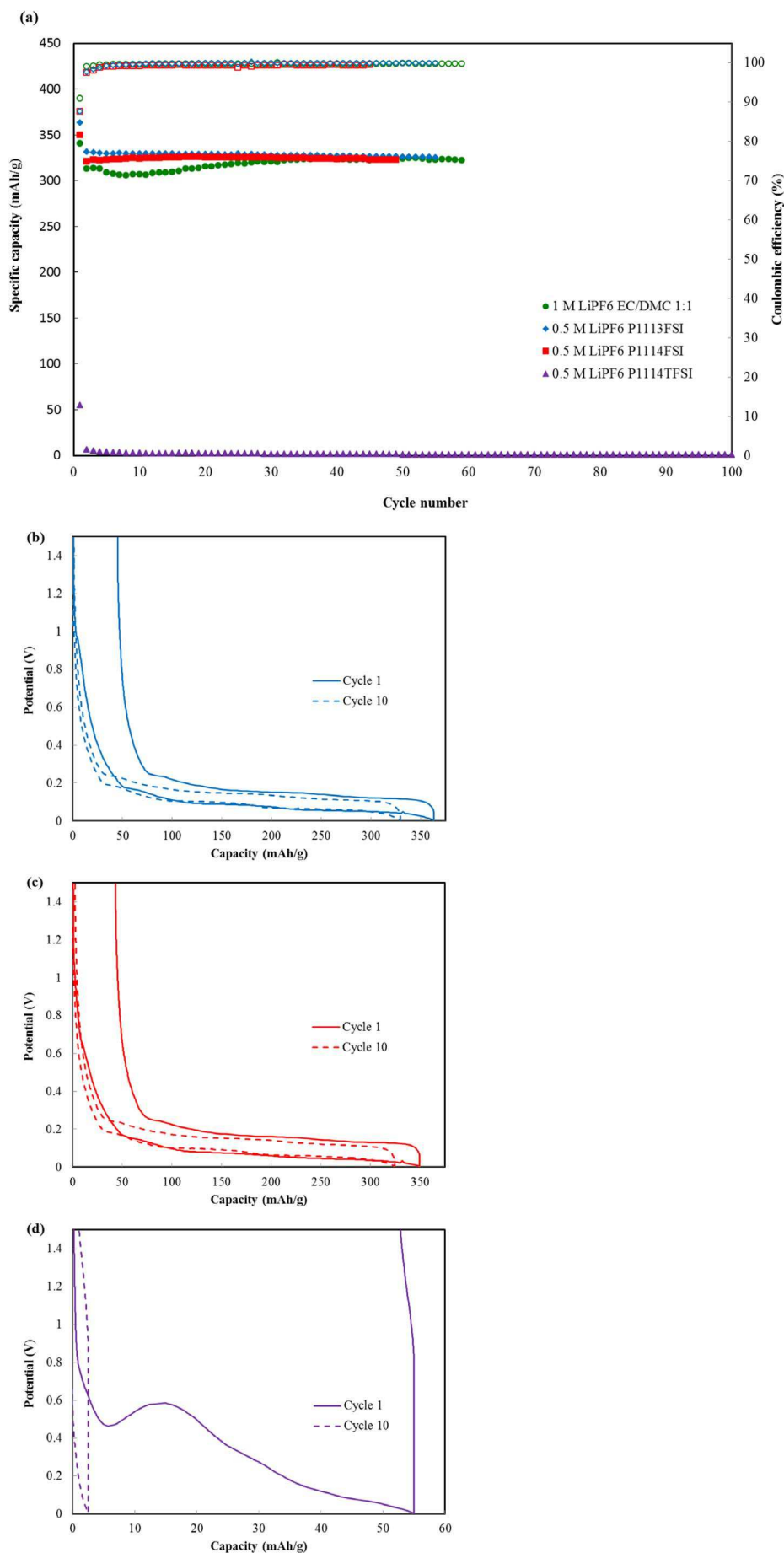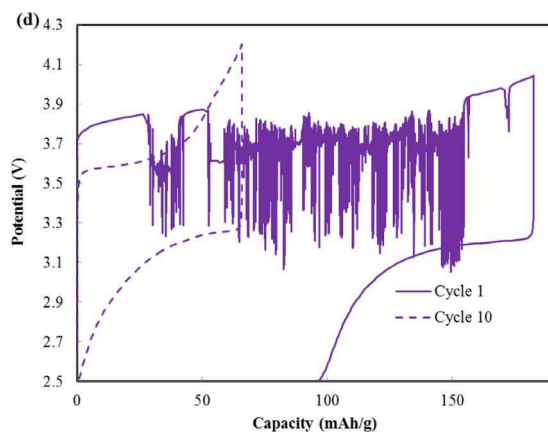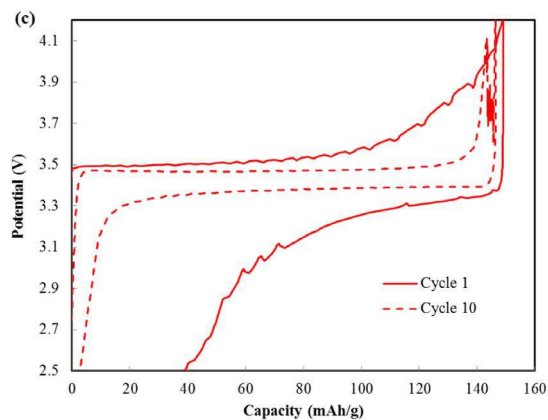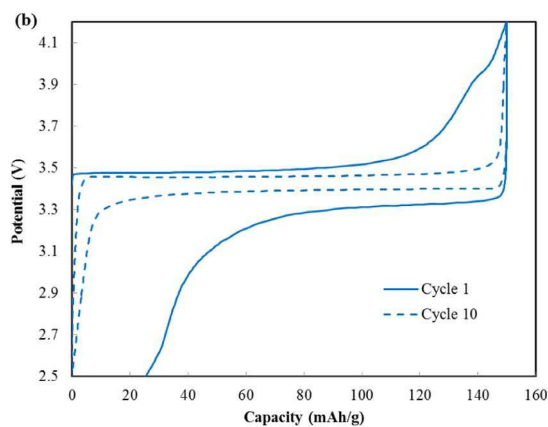**Figure 6.** (a) Discharge capacities of Li/LFP half-cells made with ionic liquid and conventional electrolytes at C/12. Open symbols are corresponding coulombic efficiencies. (b) Corresponding cycling performance curves of 0.5 M LiPF$_6$ P$_{1113}$FSI at 1st and 10th cycles. (c) Corresponding cycling performance curves of 0.5 M LiPF$_6$ P$_{111i4}$FSI at 1st and 10th cycles. (d) Corresponding cycling performance curves of 0.5 M LiPF$_6$ P$_{111i4}$TFSI at 1st and 10th cycles. P$_{1114}$FSI and P$_{1114}$TFSI refer to P$_{111i4}$FSI and P$_{111i4}$TFSI in the text.
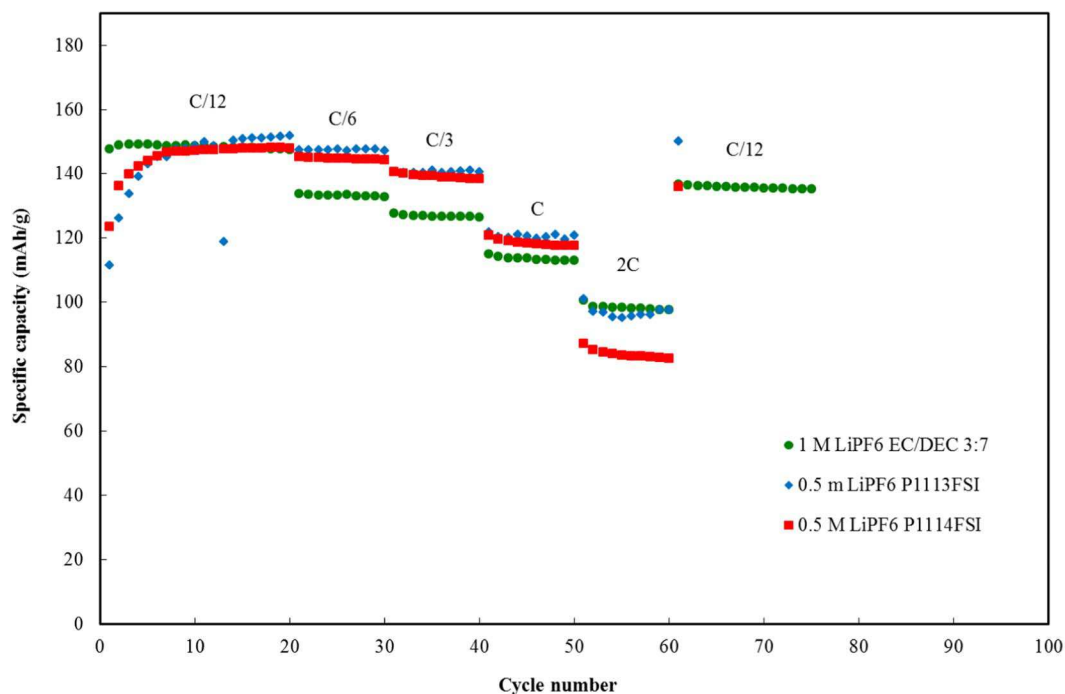
Figure 7. Rate capabilities of Li/LFP half-cells made with ionic liquid and conventional electrolytes at C/12, C/6, C/3, C and 2C. $P_{1114}FSI$ refers to $P_{111i4}FSI$ in the text.

electrolyte by ~ 15 mAh/g. The enhanced performance of the FSI^- ionic liquid electrolytes compared to conventional electrolyte could be attributed to the ability of the ionic liquids to make lithium ions more available for interaction with the cathode material.[34] The performance was still better than conventional electrolyte at 1 C rate while at 2C, 0.5 M LiPF$_6$ P$_{111i4}$FSI gave lower capacities than 0.5 M LiPF$_6$ P$_{1113}$FSI and 1 M LiPF$_6$ EC/DEC 3:7 (v/v). Half-cell made with 0.5 M LiPF$_6$ P$_{1113}$FSI recovered 100% of its original capacity at C/12 while both 0.5 M LiPF$_6$ P$_{111i4}$FSI and 1 M LiPF$_6$ EC/DEC 3:7 (v/v) suffered 7% capacity loss.

Li/LiMn$_{1.5}$Ni$_{0.5}$O$_4$ half cells.—It was anticipated from the electrochemical stability window that the ionic liquids of this study should be a successful candidate for ~ 5 V high voltage cathode LiMn$_{1.5}$Ni$_{0.5}$O$_4$, LMNO, cathode. Thus, an attempt was made to cycle Li/LiMn$_{1.5}$Ni$_{0.5}$O$_4$ with the ionic liquid electrolytes of this study. However, Li/LMNO half cells formulated with 0.5 M LiPF$_6$ P$_{1113}$FSI, 0.5 M LiPF$_6$ P$_{111i4}$FSI and 0.5 M LiPF$_6$ P$_{111i4}$TFSI failed to produce any capacity (Figure 8). This is possibly due to the reactivity of the ionic liquid electrolytes toward the active metal cations at the surface of LiMn$_{1.5}$Ni$_{0.5}$O$_4$. This could lead to chemical side-reactions
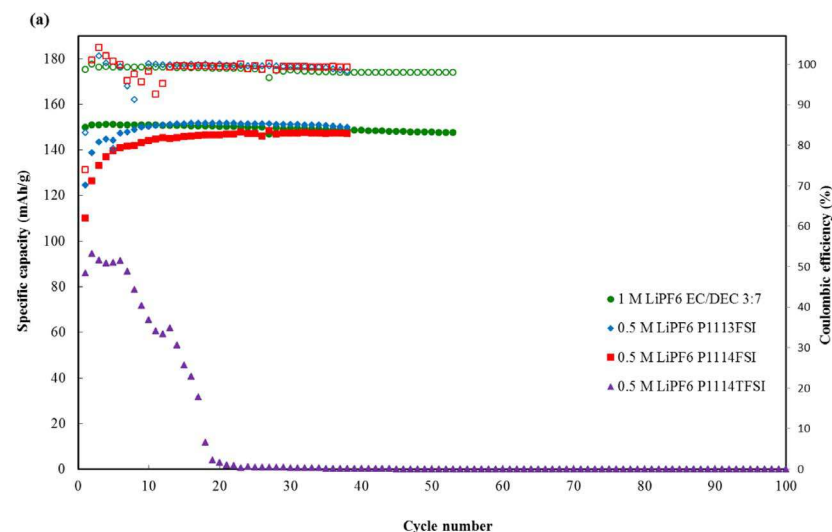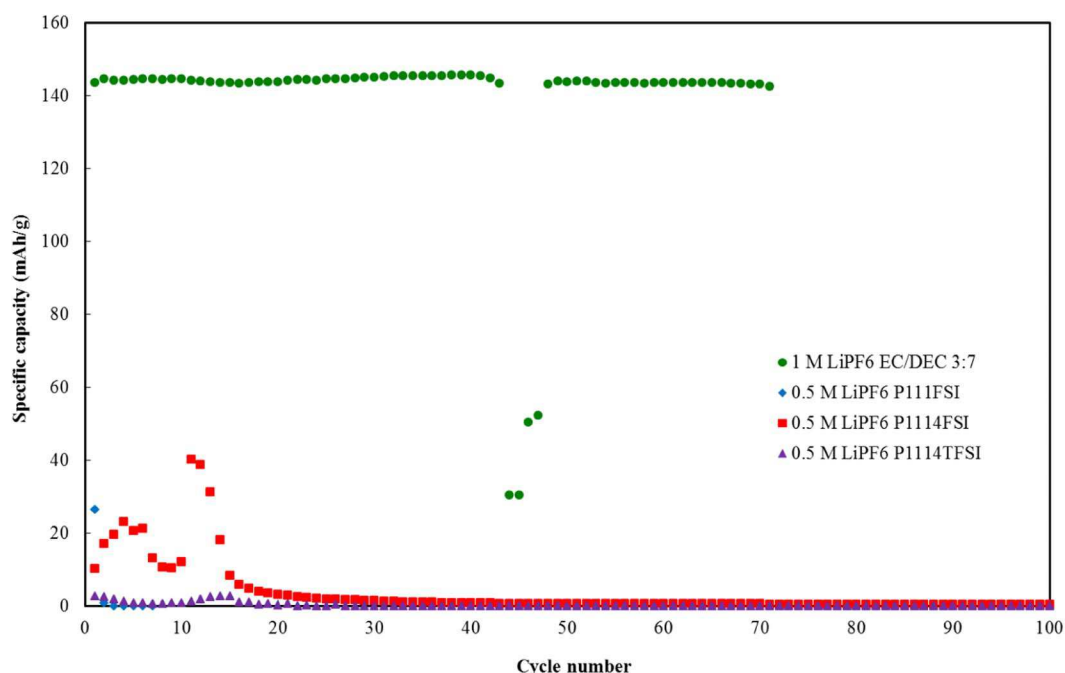

Figure 8. (a) Discharge capacities of Li/LMNO half-cells made with ionic liquid and conventional electrolytes at C/12. Open symbols are corresponding coulombic efficiencies. $P_{1114}FSI$ and $P_{1114}TFSI$ refer to $P_{111i4}FSI$ and $P_{111i4}TFSI$ in the text.

that do not give a stable Cathode-Electrolyte-Interface, (CEI), passivation layer such as in the case of carbonate electrolytes, which in turn alters the cathode performance.[35] It was previously found by our group that ionic liquid-based electrolytes can be successfully cycled with LMNO cathodes only if ethylene carbonate (EC) is added as co-solvent, possibly due to the formation of stable CEI layer on the surface of the electrode in the presence of EC and linear carbonates that protect the electrode from reacting with the ionic liquids.[36] It is widely accepted now that EC, when present with other solvents, plays a dominant role during the formation of the SEI in the initial battery cycling.[37] This, along with other superior properties such as high polarity and hence high solvation power, is the reason for using EC as a co-solvent in future work involving LMNO cathode material. It could also be beneficial to try a lithium salt of the same type as counter anion of the ionic liquid such as LiFSI or LiTFSI instead of LiPF$_6$. Gao et al. used LiTFSI salt with an ammonium based ionic liquid to successfully cycle Li/LMNO half-cell.[38] The use of additives is also a common approach; in some cases ionic liquids were shown to improve cyclability of LMNO.[39]

Conclusions

Some ionic liquids based on phosphonium cations were characterized and tested in lithium ion batteries. It was found that the size/shape of the cation and the variation in the counter anion have a significant effect on the physical and electrochemical properties and as a result battery performance. The ionic liquid with smaller cation, P$_{1113}$, was less viscous and more conductive. When combined with FSI anion it gave the best thermal, physical and electrochemical properties and the best battery performane of the ILs tested. The formulated electrolytes of the ionic liquids with 0.5 M LiPF$_6$, without having any co-solvent or additive, exhibited higher viscosities, lower conductivities and wide electrochemical windows (>6 V). The electrolytes of the FSI ionic liquids performed well with the common graphite anode in MCMB/Li half cell and common cathode LiFePO$_4$ in a Li/LFP half cell and was comparable with conventional electrolytes at slow rates, C/12 and C/6 for MCMB/Li and at slow and fast rates for Li/LFP producing ∼ 320 mAh/g and 150 mAh/g at C/12 for MCMB/Li and Li/LFP, respectively. The same electrolytes however did not perform well with the high voltage cathode (∼5 V) LiMn$_{1.5}$Ni$_{0.5}$O$_4$ in Li/LMNO half cells possibly due to the inability of ionic liquid electrolytes to form a passivation (CEI) layer at LMNO surface.

Acknowledgments

References

1. J. Arai, T. Yamaki, S. Yamauchi, T. Yuasa, T. Maeshima, T. Sakai, M. Koseki, and T. Horiba, *Journal of Power Sources*, **146**, 788 (2005).
2. O. Bitsche and G. Gutmann, *Journal of Power Sources*, **127**, 8 (2004).
3. Y. S. Jung, A. S. Cavanagh, A. C. Dillon, M. D. Groner, S. M. George, and S. H. Lee, *Journal of the Electrochemical Society*, **157**, A75 (2010).
4. S. Menkin, D. Golodnitsky, and E. Peled, *Electrochemistry Communications*, **11**, 1789 (2009).
5. J. Patra, P. P. Dahiya, C.-J. Tseng, J. Fang, Y.-W. Lin, S. Basu, S. B. Majumder, and J.-K. Chang, *Journal of Power Sources*, **294**, 22 (2015).
6. S. V. Sazhin, M. K. Harrup, and K. L. Gering, *Journal of Power Sources*, **196**, 3433 (2011).
7. J. Hassoun, A. Fernicola, M. A. Navarra, S. Panero, and B. Scrosati, *Journal of Power Sources*, **195**, 574 (2010).
8. V. Borgel, E. Markevich, D. Aurbach, G. Semrau, and M. Schmidt, *Journal of Power Sources*, **189**, 331 (2009).
9. M. Galiński, A. Lewandowski, and I. Stepniak, *Electrochimica Acta*, **51**, 5567 (2006).
10. J. Mun, Y. S. Jung, T. Yim, H. Y. Lee, H.-J. Kim, Y. G. Kim, and S. M. Oh, *Journal of Power Sources*, **194**, 1068 (2009).
11. J. Mun, S. Kim, T. Yim, J. H. Ryu, Y. G. Kim, and S. M. Oh, *Journal of the Electrochemical Society*, **157**, A136 (2010).
12. J. Mun, T. Yim, C. Y. Choi, J. H. Ryu, Y. G. Kim, and S. M. Oh, *Electrochemical and Solid-State Letters*, **13** A109 (2010).
13. L. Zhao, J.-i. Yamaki, and M. Egashira, *Journal of Power Sources*, **174**, 352 (2007).
14. S. Zhang, N. Sun, X. He, X. Lu, and X. Zhang, *Journal of Physical and Chemical Reference Data*, **35**, 1475 (2006).
15. A. S. Best, A. I. Bhatt, and A. F. Hollenkamp, *Journal of The Electrochemical Society*, **157**, A903 (2010).
16. A. Fernicola, B. Scrosati, and H. Ohno, *Ionics*, **12**, 95 (2006).
17. K. Tsunashima, Y. Sakai, and M. Matsumiya, *Electrochemistry Communications*, **39**, 30 (2014).
18. G. M. A. Girard, M. Hilder, H. Zhu, D. Nucciarone, K. Whitbread, S. Zavorine, M. Moser, M. Forsyth, D. R. MacFarlane, and P. C. Howlett, *Physical Chemistry Chemical Physics*, **17**, 8706 (2015).
19. M. Hilder, G. N. A. Girard, K. Whitbread, S. Zavorine, M. Moser, D. Nucciarone, M. Forsyth, D. R. MacFarlane, and P. C. Howlett, *Electrochimica Acta*, , **202**, 100 (2016).
20. R. Younesi, G. M. Veith, P. Johansson, K. Edstrom, and T. Veggea, *Energy Environ. Sci.*, **8**, 1905 (2015).
21. N. Salem, L. Nicodemou, Y. Abu-Lebdeh, and I. J. Davidson, *Journal of The Electrochemical Society*, **159**, A172 (2011).
22. M. Kunze, M. Montanino, G. B. Appetecchi, S. Jeong, M. Schönhoff, M. Winter, and S. Passerini, *The Journal of Physical Chemistry A*, **114**, 1776 (2010).
23. C. F. Poole, *Journal of Chromatography A*, **1037**, 49 (2004).
24. M. Kerner, N. Plylahan, J. Scheers, and P. Johansson, *Physical Chemistry Chemical Physics*, **17**, 19569 (2015).
25. K. Ghandi, *Green and Sustainable Chemistry*, Vol. **4**, No. 1 (2014).
26. K. Tsunashima and M. Sugiya, *Electrochemistry Communications*, **9**, 2353 (2007).
27. H. Matsumoto, M. Yanagida, K. Tanimoto, M. Nomura, Y. Kitagawa, and Y. Miyazaki, *Chem. Lett.*, **8**, 922 (2000).
28. W. Beichel, Y. Yu, G. Dlubek, R. Krause-Rehberg, J. Pionteck, D. Pfefferkorn, S. Bulut, D. Bejan, C. Friedrich, and I. Krossing, *Physical Chemistry Chemical Physics*, **15**, 8821 (2013).
29. C.-H. Yim, J. Tam, H. Soboleski, and Y. Abu-Lebdeh, *J. Electrochem. Soc.*, **164**(6), A1002 (2017).
30. G. B. Appetecchi, M. Montanino, D. Zane, M. Carewska, F. Alessandrini, and S. Passerini, *Electrochim. Acta*, **54**, 1325 (2009).
31. E. Paillard, Q. Zhou, W. A. Henderson, G. B. Appetecchi, M. Montanino, and S. Passerini, *Journal of The Electrochemical Society*, **156**, A891 (2009).
32. A. Guerfi, S. Duchesne, Y. Kobayashi, A. Vijh, and K. Zaghib, *Journal of Power Sources*, **175**, 866 (2008).
33. K. R. Seddon, A. Stark, and M.-J. Torres, *Pure Appl. Chem.*, **72** (12), 2275 (2000).
34. "Electrolytes for Lithium and Lithium-Ion Batteries", edited by Richard T. Jow, Kang Xu, Oleg Borodin, and Makoto Ue, Springer, 2014.
35. J. Mun, T. Yim, K. Park, J. H. Ryu, Y. G. Kim, and S. M. Oh, *Journal of The Electrochemical Society*, **158**, A453 (2011).
36. N. Salem and Y. Abu-Lebdeh, *Journal of The Electrochemical Society*, **161**, A1593 (2014).
37. K. Xu and A. von Cresce, *Journal of Materials Chemistry*, **21**, 9849 (2011).
38. X.-W. Gao, C.-Q. Feng, S.-L. Chou, J.-Z. Wang, J.-Z. Sun, M. Forsyth, D. R. MacFarlane, and H.-K. Liu, *Electrochimica Acta*, **101**, 151 (2013).
39. S.-Y. Bae, W.-K. Shin, and D.-W. Kim, *Electrochimica Acta*, **125**, 497 (2014).